Termination of the Carbomethoxyisopropyl Radical, a Poly(methyl methacrylate) Model, in the Presence of Copper Complexes and Proton Donors

Julian Sobieski, Sajjad Dadashi Silab, Lucas Thevenin, Krzysztof Matyjaszewski, Christophe Fliedel, Rinaldo Poli

Termination of the carbomethoxyisopropyl radical, a poly(methyl methacrylate) model, in the presence of copper complexes and proton donors

Julian Sobieski,[†] Sajjad Dadashi Silab,[†] Lucas Thevenin,[‡] Krzysztof Matyjaszewski,[†] Christophe Fliedel,[‡]* Rinaldo Poli[‡§]**

[†] Department of Chemistry, Carnegie Mellon University, 4400 Fifth Avenue, Pittsburgh, PA 15213, United States.

[‡] CNRS, LCC (Laboratoire de Chimie de Coordination), Université de Toulouse, UPS, INPT, 205 Route de Narbonne, BP 44099, F-31077, Toulouse Cedex 4, France.

[§] Institut Universitaire de France, 1, rue Descartes, 75231 Paris Cedex 05, France.

KEYWORDS. Copper; Organocopper(II) Complexes; Methacrylate Radical; Catalyzed Radical Termination; Reductive Radical Termination; Atom Transfer Radical Polymerization (ATRP).

ABSTRACT.

The termination processes of the tertiary carbomethoxyisopropyl radical, (COOMe)$Me_2C^{\bullet}$, have been investigated by ^{1}H NMR under a variety of conditions. The radical was generated by thermal activation of dimethyl 2,2'-azobis(2-methylpropionate) (V-601) and by bromine atom transfer from methyl 2-bromoisobutyrate (MBiB) to Cu^I/L activators (80 °C in CD_3CN, Cu^I = $[Cu(MeCN)_4]^+BF_4^-$, L = tris[2-(dimethylamino)ethyl]amine (Me_6TREN), tris(2-pyridyl-methyl)amine (TPMA), 2,2'-bipyridine (bpy); 75 °C in C_6D_6; Cu^I = CuBr, L = Me_6TREN, TPMA) in the presence of various additives: the Cu^I/L complex (for the V-601 decomposition), Cu^0 (in C_6D_6) and/or proton/deuteron donors (CH_3OH, CD_3OD, $Et_3NH^+BF_4^-$). The investigation has allowed an assessment of the relative contributions of the Cu^I/L-catalyzed radical termination (CRT) and of the reductive radical termination (RRT) to the spontaneous bimolecular radical terminations (RT) of the diffused radicals. The investigation also allowed reassessing the product distribution for the RT of the diffused and caged radicals obtained from the thermal activation of V-601. Both CRT and RRT were found to be minor but not negligible when the radical is slowly produced from V-601. The more rapid radical generation by atom transfer from MBiB maintains RT and CRT and decreases the impact of RRT. The catalytic activity in CRT decreases in the order Cu^I/TPMA > Cu^I/Me_6TREN and is less prominent in C_6D_6 than in CD_3CN, whereas the RRT activity increases in the order Cu^I/TPMA < Cu^I/Me_6TREN and is less prominent in CD_3CN. DFT calculations validate the principle that CRT occurs *via* formation of a latent organometallic (COOMe)Me_2C-Cu^{II}/L intermediate.

Introduction

Methacrylate monomers are of great interest for the polymer industry and are typically polymerized by the radical mechanism. Due to the persistent radical effect[1] and/or rapid degenerative transfer, a number of different methods, globally referred to as "Reversible Deactivation Radical Polymerization" (RDRP),[2, 3] have been developed to build elaborate macromolecular architectures that include poly(meth)acrylate blocks with targeted molecular weight, low dispersities and high chain-end functionalities. We are particularly interested in metal-catalyzed radical polymerization, also known as "Atom Transfer Radical Polymerization" (ATRP),[4-9] where a metal catalyst (Mt^x/L) activates a halogen-terminated dormant species (P_n-Y) to reversibly generate the active radical chain ($P_n^{\bullet}$) and a higher oxidation state complex (Y-Mt^{x+1}/L), which acts as deactivator (Scheme 1). Learning how to diminish the contribution of the inevitable terminations to the lowest possible extent is primordial to maintain the highest possible degree of chain-end fidelity, which is of utmost importance for the engineering of more elaborate structures (*e.g.* multiblocks, grafts, brushes, functionalized surfaces, bioconjugates, *etc.*).[3, 10-12] Amongst all possible catalysts, those based on the Cu^I/Cu^{II} redox pair have attracted the greatest attention because of the ready availability and low cost of the metal, wide ligand choice, and adaptability to diverse operating conditions. The catalytic activity of these systems, as reflected by the ATRP equilibrium constant value (K_{ATRP}), is strongly ligand and medium dependent.[13-15] Systems up to one billion times more active than the originally employed Cu^I/bpy catalyst have recently been developed.[16-19]

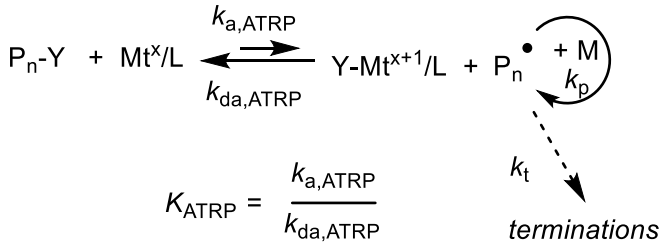

Scheme 1. Atom transfer equilibrium in metal-catalyzed radical polymerization (ATRP). P_n = growing radical chain, M = monomer, Mt^x/L = catalyst comprising a metal (Mt) in oxidation state x and ligands (/L).

The K_{ATRP} increase, however, is paralleled by an increased tendency for the Cu^I/L species to directly trap the radical chain and generate an organometallic dormant species, P_n-Cu^{II}/L, at least within the family of C_3-symmetric catalysts supported by substituted tris(pyridylmethyl)amine (TPMA) ligands.[20-22] A reversible chain trapping by a metal complex Mt^x/L, yielding P_n-Mt^{x+1}/L (Scheme 2), if uncontaminated by other side processes, also provides a mechanism for controlled chain growth, known as "Organometallic-Mediated Radical Polymerization" (OMRP).[23, 24] However, recent work has shown that the organometallic P_n-Cu^{II}/L species may also lead to an additional radical termination mechanism, termed "Catalyzed Radical Termination" (CRT, also highlighted in Scheme 2).[25, 26] This pathway consists of the reaction between paramagnetic P_n-Cu^{II}/L and a second radical chain, $P_m^\bullet$, regenerating the Cu^I/L catalyst and yielding termination products. To date, the CRT phenomenon has only been evidenced for polyacrylate radical chains, whereas polymethacrylates and polystyrene were shown not to suffer from this additional termination pathway.[21]

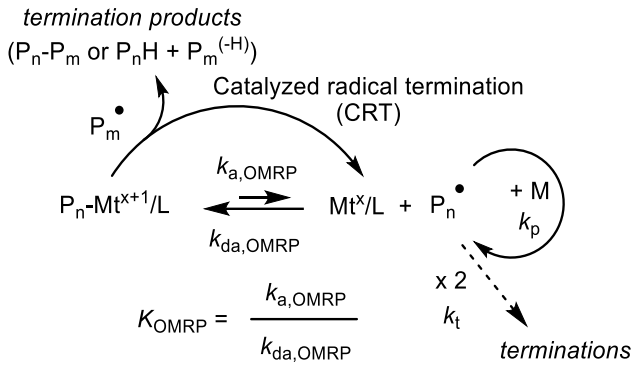

Scheme 2. Reactions between an organic radical and a metal complex leading to an organometallic dormant species and subsequent quenching of the latter by a second radical in CRT.

An additional radical termination process that potentially interferes with a controlled chain growth is reductive radical termination (RRT, Scheme 3),[27] whereby the $P_n^{\bullet}$ radical is selectively quenched to form the saturated P_m-H product by addition of an electron from Mt^x/L and a proton from an acidic H-Z molecule, yielding the oxidized ZMt^{x+1}/L complex. Radical reduction to saturated alkanes in the presence of proton donors is a well-known phenomenon that, specifically, has been described in some details for copper(I) in an aqueous environment.[28-30] The process can in principle occur by one of three independent pathways: (*i*) outer-sphere proton-coupled electron transfer (OSPCET); (*ii*) inner-sphere proton-coupled electron transfer (ISPCET); or (*iii*) radical trapping followed by protonation (labelled OMRP because the organometallic intermediate is also the dormant species of organometallic-mediated radical polymerization).

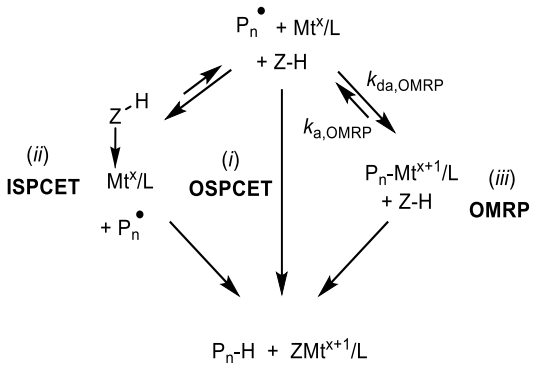

Scheme 3. Reductive radical termination (RRT).

In macromolecular chemistry, this phenomenon has been highlighted for polyacrylate chains by S. Yamago *et al.*, who demonstrated that the activation of a well-defined PMA-Br ATRP macroinitiator by a Cu^I/Me_6TREN system (Me_6TREN = tris[2-(dimethylamino)ethyl]amine) in the absence of monomer leads to the selective formation of PMA-D when CD_3OD is present.[31] Other investigations of radical macroinitiators, namely PSt-Br and PMA-Br by atom transfer to Cu^I/L complexes[26, 32] or the TERP macroinitiators P_n-TeR (P_n = PSt, PMA, PMMA; R = Me, Ph) by thermal or photochemical activation,[33-35] on the other hand, were conducted in the absence of proton donors and have revealed the intervention of CRT only for the PMA-Br chains activated by atom transfer.[32] An anomalous increase of disproportionation products for the TERP macroinitiators in high-viscosity solvents[35] was attributed to a competing β-H transfer reaction to the tellanyl radical in the $\{P_n^{\bullet},TeR^{\bullet}\}$ radical cage.[36]

In order to more clearly understand the impact of CRT and RRT in ATRP, we have started to investigate the termination of model radicals, generated by different methods, under a variety of conditions (ligand, solvent, amount and nature of an external proton donor). We have recently reported on the termination of the cyanoisopropyl radical,[37] which is a model of a methacrylonitrile polymer chain. This radical was obtained by thermal activation of azobis(isobutyronitrile) (AIBN) in the absence of monomer and was allowed to spontaneously decompose, either in CD_3CN in the

presence of $[Cu(L)]^+$ or in C_6D_6 in the presence of $CuBr/Cu^0/L$ (*i.e.* conditions close to those used in the previous termination studies of ATRP macroinitiators[26, 31, 32]) and either H_2O, CH_3OH, their deuterated analogues, or Et_3NH^+ as proton donors. The most important lessons learned from that study are that $Me_2(CN)C^\bullet$ can indeed interact with the Cu^I/L complex, most favorably in the ligand order Me_6TREN > TPMA >> bpy (no interaction), although this occurs preferentially via the N atom to afford a ketiminate derivative $[L/Cu^{II}\text{-}N{=}C{=}CMe_2]^+$. This interaction does not lead to any detectable CRT, whereas RRT occurs extensively by protonolysis of the Cu-radical adduct (*iii* in Scheme 3) and is promoted by the proton donor acidity; the alternative coupled proton-electron transfer pathways (*i* and *ii* in Scheme 3) do not appear to significantly contribute.

In the present contribution, we report a related investigation on the termination of the carbomethoxyisopropyl radical ($Me_2C^\bullet(COOMe)$, a polymethacrylate chain model). This radical has been generated either by thermal decomposition of a diazo initiator (V-601) or by atom transfer activation from methyl 2-bromoisobutyrate (MBiB), see Scheme 4. The advantage of the diazo initiator decomposition is to allow control experiments in the absence of the copper complex and is thus useful for comparing the two different activation methods. The $Me_2C^\bullet(COOMe)$ termination, after generation from V-601 under various conditions, has previously been described.[36, 38] Terminations of the same radical were also investigated following the photochemical activation of $Me_2C(COOMe)$-TeR, (R = Ph,[33] Me[35]), but the generation by atom transfer from MBiB, allowing for the possible intervention of CRT and RRT, has not been previously reported. An additional advantage of the atom transfer activation method from MBiB by Cu^I/L complexes is that no side-reactivity is possible for the organic radical within the $\{Me_2(COOMe)C^\bullet, BrCu^{II}/L\}$ radical cage prior to diffusion to the bulk, contrary to the caged radical obtained from $Me_2C(COOMe)$-TeR. Comparison of the results with those of the related

cyanoisopropyl radical reveals striking difference in the binding mode to the Cu^{I} center and in the effect of this binding on the radical termination.

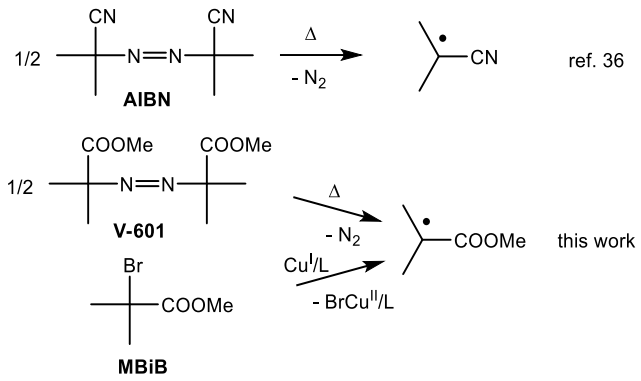

Scheme 4. Used strategies for radical generation.

Results and Discussion

All possible transformations for this radical are shown in Scheme 5. Both the spontaneous radical termination (RT) and the catalyzed radical termination (CRT) lead to either the radical dimer (dimethyl tetramethylsuccinate, indicated as R-R) by combination (Comb) or a 1:1 mixture of methyl methacrylate (MMA) and the saturated product (methyl isobutyrate, indicated as R-H) by disproportionation (Disp). However, the amount of MMA relative to R-H may be reduced by further reaction with $R^{\bullet}$, leading to oligomeric radicals, which may terminate once again by either Comb or Disp, spontaneously or catalytically. In addition, RRT, if present, leads to the specific formation of R-H. Hence, the R-H/MMA ratio may be greater than 1 as a result of oligomerization and/or RRT.

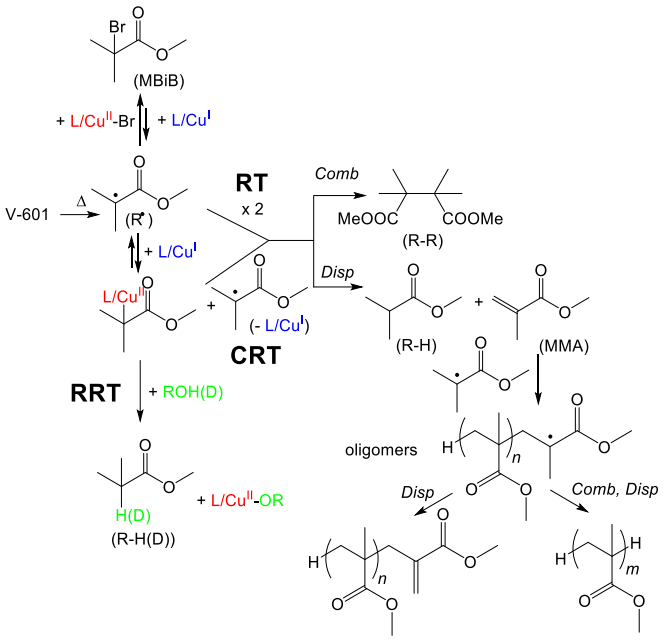

Scheme 5. Possible termination processes for the carbomethoxyisopropyl radical.

The relationship between the observed products and their genesis is schematically illustrated in Scheme 6. Demonstrating the presence of CRT and RRT is consequently difficult, but at least qualitative indications may be provided by comparing the product distributions obtained in the presence of variable amounts of H^+ or D^+ donors and by comparing these with those of control experiments carried out in the absence of copper complexes (only when using the diazo initiator). Specifically, the relative proportions of Comb and Disp (equations 1 and 2) originating from RT is available from the experiments carried out in the absence of copper complex (no CRT) and proton donor (no RRT). The results obtained in the presence of copper complex without proton donor can assess the presence of CRT, if this leads to a significant change of the Comb/Disp ratio. Finally, the presence of RRT can be assessed from the effect of proton donors on the product distribution (comparison of equations 2 and 3). The experimental procedures used for the decomposition experiments are described in the SI (section S1) and the relative amounts of the

various products were determined by ^{1}H NMR integration as detailed in section S2, Figure S1 and Figure S2.

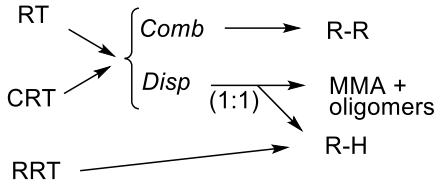

$$\frac{\%(R\text{-}R)}{2} = \%\ Comb \qquad (1)$$

$$\%(MMA) + \%\ (oligomers) = \%\ Disp \qquad (2)$$

$$\%(R\text{-}H) = \%\ Disp + \%\ RRT \qquad (3)$$

Scheme 6. Relationship between the termination mechanism and the resulting products.

a. Terminations from V-601.

These experiments, like those previously reported for the termination of the cyanopropyl radical,[37] were conducted in both CD_3CN and C_6D_6 (see section S1 for the experimental procedures). In order to make the results comparable, the experimental conditions were also the same, namely using a 1:2 $[Cu(MeCN)_4]^+BF_4^-$/L ratio in CD_3CN and a 1:4:1.7 CuBr/Cu^0/L ratio in C_6D_6, (except when otherwise noted), using L = Me_6TREN or TPMA. The speciation of the copper complex in CD_3CN features $[Cu^I(L)]^+$ as the dominant species, since disproportionation of Cu^I to Cu^{II} and Cu^0 is negligible in this solvent and is further disfavored by the excess L.[39] The speciation of the CuBr/Cu^0/L system in C_6D_6, on the other hand, is less well defined.[40]

a1. In CD_3CN.

The results of the experiments carried out in CD_3CN are collected in Table 1. Triplicate runs were carried out for a few experiments. In those cases, average parameters together with their standard deviations are also shown. In all cases, the V-601 decomposition was nearly complete, as expected from the known half-life of this initiator,[41, 42] after 8 h at 80°C. The oligomer fraction

could not be obtained with precision from the NMR spectra because it could only be estimated by difference (see details in the SI, section S2) and is therefore subjected to the propagation of integration errors. In the absence of RRT, which would produce additional R-H relative to the termination by Disp, this amount was fixed as the difference between the R-H and MMA amounts (equation 2).

Table 1. Product distribution from the termination of carbomethoxyisopropyl radicals generated by activation of V-601 in CD_3CN under various conditions.[a]

Entry	Cu^I/R	L	Additive (equiv per R)	V-601 conv.	% R-R	% R-H (% D)	$2\frac{R-H}{R-R}$ [b]	MMA	%RRT
1	0	-	-	97.75	49.31	25.35	1.03	0.89	
				99.01	50.10	24.95	1.00	0.60	
				98.47	50.12	25.05	1.00	0.75	
					49.8±0.4[c]	*25.1±0.2*[c]	*1.01±0.01*[c]	*0.8±0.1*[c]	
2	0	-	CH_3OH (100)[d]	96.98	49.39	25.30	1.02	0.84	
3	0	-	CD_3OD (100)[d]	95.60	49.28	25.36 (0)	1.03	0.94	
4	1[e]	Me_6TREN	-	98.84	46.13	26.94	1.17	0.92	
				99.09	48.94	25.53	1.04	0.69	
				98.89	49.49	25.26	1.02	0.89	
					48.2±1.4[c]	*25.9±0.7*[c]	*1.08±0.06*[c]	*0.8±0.1*[c]	
5	1[f]	TPMA	-	99.59	44.43	27.78	1.25	0.71	
				99.20	47.30	26.35	1.11	0.76	
				99.64	47.73	26.14	1.09	0.81	
					46.5±1.4[c]	*26.8±0.7*[c]	*1.15±0.06*[c]	*0.76±0.03*[c]	
6	1[e]	Me_6TREN	CH_3OH (100)[d]	90.01	45.35	28.37	1.25	1.27	2.1
7	1[e]	Me_6TREN	CD_3OD (100)[d]	98.37	46.55	27.32 (0)	1.17	1.12	1.2
8	1[e]	Me_6TREN	$Et_3NH^+PF_6^-$ (1)[g]	96.86	47.86	26.32	1.10	0.81	0.5
9	1[e]	Me_6TREN	$Et_3NH^+PF_6^-$ (20)[g]	98.06	41.33	32.79	1.58	0.87	6.9
10	1[f]	TPMA	CH_3OH (100)[d]	99.38	48.11	26.11	1.09	0.77	0.3
11	1[f]	TPMA	CD_3OD (100)[d]	99.38	48.25	25.92 (0)	1.07	0.82	0.1
12	1[f]	TPMA	$Et_3NH^+PF_6^-$ (1)[g]	97.38	46.55	27.70	1.19	0.74	1.9
13	1[f]	TPMA	$Et_3NH^+PF_6^-$ (20)[g]	96.41	28.46	45.65	3.21	0.88	19.8

[a] Conditions: [V-601] = 5 mg (0.022 mmol) in 0.7 mL of CD_3CN, 8 h at 80°C. [b] Ratio of the two C*H*$_3$C resonances (see SI), hence equivalent to the molar ratio of radicals leading to each product. [c] Average and standard deviation. [d] CH_3OH or CD_3OD (0.18 mL, 4.4

mmol). [e] $[Cu(MeCN)_4]BF_4$ (13.8 mg, 0.044 mmol) and Me_6TREN (24 μL, 20.3 mg, 0.088 mmol). [f] $[Cu(MeCN)_4]BF_4$ (13.8 mg, 0.044 mmol) and TPMA (25.6 mg, 0.088 mmol). [g] $Et_3NH^+PF_6^-$ (10.9 mg, 0.044 mmol, 1 eq.) or (217.5 mg, 0.88 mmol, 20 eq.).

The control experiments carried out in the absence of copper complex and proton donor (entry 1) show the essential equivalence of the combination (R-R product, 49.8±0.4%) and disproportionation (sum of R-H, MMA and oligomers) modes of termination. This result agrees with a previous investigation, which reported Disp/Comb ratio in the range 0.75 – 1.50 as a function temperature in low-viscosity solvents (*i.e.* C_6D_6 and DMSO-d_6).[38] In particular, that investigation showed that the Disp/Comb ratio depends on the microviscosity,[43] as this parameter affects the ability of the radical pair to separate from the radical cage. In addition, it was shown that the Disp/Comb ratio for the caged radical pair is slightly smaller and less viscosity-dependent than for the diffused radical pair.[38] In order to more properly compare our results with those reported in the literature, which did not include CD_3CN as a solvent, we have proceeded to measure the CD_3CN diffusion constant at 80°C by DOSY NMR, allowing to calculate the microviscosity at this temperature. However, technical modifications of the reported procedure[38, 43] were needed to eliminate convection, which is important even in the absence of tube spinning and found to significantly affect the measurements (see SI, section S1 for the experimental details and section S3 for the comprehensive results). Using this method, the measured diffusion constant of CHD_2CN in CD_3CN at 25°C was $5.0 \cdot 10^{-9}$ m^2 s^{-1}, in good agreement with the literature value of $4.17 \cdot 10^{-9}$ m^2 s^{-1} for the diffusion of CH_3CN in CD_3CN.[44] The measured value of the CD_3CN microviscosity at 80 °C is reported in Table 2.

Table 2. Comparison of the Disp/Comb ratios measured for the decomposition of V-601 under different conditions.

Solv/Temp (°C)	η_{micro} [mPa s]	Disp/Comb	Ref.

CD_3CN/80°C	0.160 [a]	1.01±0.01	This work
C_6D_6/75°C	0.232 [a]	0.73±0.01	This work
C_6D_6/80°C	0.222 [a,b]	0.79	[38]

[a] Determined by DOSY NMR (see SI, section S3). [b] This value was reported as 0.081 in ref. [38].

The addition of proton donors (CH_3OH or CD_3OD) in the absence of copper does not significantly change the product distribution, as might be expected (entries 2-3 in Table 1). The introduction of Cu^I/L in the absence of proton donor (runs 4 and 5) has a very minor effect, which is perhaps most clearly notable in a slight increase of the Disp/Comb ratio from 1.01±0.01 to 1.08±0.06 for L = Me_6TREN and 1.15±0.06 for L = TPMA. This suggests the presence of a slight contribution of CRT, preferentially leading to the Disp products. It is appropriate to remind that Cu^I/TPMA was shown[32] to have greater CRT activity than Cu^I/Me_6TREN in CD_3CN for the termination of polyacrylate radicals, where the effect of CRT is much more important, and the CRT of the polyacrylate radicals was shown to strongly favor Disp. Note that, in all the above experiments, no RRT may occur because there is either no reducing copper complex, or no proton donor, or neither. The percent of oligomers, calculated from equation 2, was essentially the same in all these experiments, averaging 25.0±0.7%.

The introduction of both copper complex and proton donor additives gave the results collected in entries 6-13 (Table 1). For these experiments, the fraction of oligomers in the product distribution was imposed as equal to the average from the above control experiments, namely 25.0%, and the other measured products were scaled to the remaining 75%. In most cases, the product distribution remained very close to those recorded for the control experiments. The % Disp was calculated from equation 2 (Scheme 6) and the contribution of RRT could then be evaluated by application of equation 3. Note that the application of equation 3 to all control experiments

(entries 1-5), for which RRT cannot take place in principle, yields an average % RRT equal to (0.0±0.7), reassuring us about the self-consistency of the method. For the Me_6TREN system, a slight increase of the $2\frac{R-H}{R-R}$ ratio was observed from 1.08±0.06 in the absence of proton additive to 1.25 with CH_3OH (100 equiv., entry 6) and 1.17 with CD_3OD (100 equiv., entry 7), leading to the calculation of % RRT values that slightly exceed the standard deviation value. However, no unambiguous D incorporation could be detected from the resonance of the saturated product for the experiment in entry 7. In the presence of the stronger acid $Et_3NH^+PF_6^-$, the distribution is not significantly changed when using it in a stoichiometric amount (0.5% of calculated RRT, *i.e.* within the experimental error, entry 8), but a much greater amount of R-H is produced with a 20-fold excess (5.6% of RRT, entry 9). For the TPMA system, the introduction of CH_3OH or CD_3OD (100 equiv.) results again in a very small calculated % RRT, within the noise level (entries 10-11) and no D incorporation was noticeable when using CD_3OD. However, the addition of $Et_3NH^+PF_6^-$ had a more noticeable effect in the calculated % RRT (1.9 with the stoichiometric amount, entry 12, and 19.8 with a 20-fold excess, entry 13). These data suggest, therefore, that an interaction between the Cu^I/L complexes and the carbomethoxyisopropyl radical does take place. However, this interaction is very weak and leads to a minor impact of both CRT and RRT. In comparison, the previously reported termination of the cyanoisopropyl radical, which was also generated by the thermal decomposition of an azo initiator (AIBN, see Scheme 4), led to extensive RRT in the presence of both Cu^I/Me_6TREN and methanol and to extensive D incorporation from CD_3OD.

a2. In C_6D_6.

The results of these experiments are collected in Table 3. The reaction time and temperature (8 h at 75°C) led in all cases to V-601 conversions in excess of 70%. The control experiment (entry 14) gave a significantly greater extent of combination (57.7±0.2%) than the same experiment in

CD_3CN, resulting in a smaller Disp/Comb ratio (0.73±0.01). This value agrees quite well with that reported by Yamago *et al.* under very similar conditions[38] (see Table 2). The lower Disp/Comb ratio observed in C_6D_6 relative to CD_3CN, under conditions in which CRT and RRT are absent, merits a deeper analysis. According to the previous contribution,[38] a greater microviscosity should lead to an increase of the Disp/Comb ratio. For instance, the reported values at 80°C are 44:56 or 0.79 in C_6D_6 (η = 0.081[38] or 0.222 as remeasured by us, see Table 2 and SI), 55:45 or 1.22 in DMSO-d_6 (η = 0.38[38]) and 55:45 or 1.22 in PEG-400 (η = 0.63[38]). However, we find that the Disp/Comb ratio is greater in CD_3CN than in C_6D_6, even though its microviscosity is smaller (Table 2 and SI). Therefore, the conclusion reached in the previous contributions[38] on the Disp/Comb dependence on microviscosity does not appear to apply to our new measurements, implying that the change of the Disp/Comb ratio from CD_3CN to C_6D_6 is not only affected by this single physical parameter. A deeper investigation of this effect, however, is beyond the scope of the present contribution.

Table 3. Product distribution from the termination of carbomethoxyisopropyl radicals generated by activation of V-601 in C_6D_6 under various conditions.[a]

Entry	Cu^I/R	Additive (equiv per R)	L	V-601 conv.	% R-R	% R-H (% D)	$2\frac{R-H}{R-R}$ [b]	MMA	%RRT
14	0	-	-	72.89	57.36	21.32	0.74	1.26	
				74.88	58.07	20.96	0.72	1.05	
				74.92	57.69	21.15	0.73	1.04	
					57.7±0.2[c]	*21.2±0.1*[c]	*0.73±0.01*[c]	*1.12±0.10*[c]	
15	0	CH_3OH (40)[d]	-	83.37	59.01	20.50	0.70	0.89	
16	0	CD_3OD (40)[d]	-	76.52	58.99	20.51 (0)	0.70	1.06	
17	0.5[e]	-	Me_6TREN	84.16	58.34	20.83	0.71	1.52	
				76.10	57.45	21.28	0.74	1.03	
				76.35	55.85	22.08	0.79	0.95	
					57.2±0.9[c]	*21.4±0.5*[c]	*0.75±0.03*[c]	*1.2±0.2*[c]	
18	0.5[f]	-	TPMA	72.49	56.43	21.78	0.77	1.13	
				72.90	56.67	21.67	0.76	1.13	
				75.78	57.36	21.32	0.74	0.80	
					56.8±0.4[c]	*21.6±0.2*[c]	*0.76±0.01*[c]	*1.0±0.2*[c]	
19	0.5[e]	CH_3OH (40)[d]	Me_6TREN	89.82	47.64	32.43	1.36	0.62	12.2
20	0.5[e]	CD_3OD (40)[d]	Me_6TREN	80.31	50.63	28.76 (0)	1.14	1.01	7.4
21	0.5[f]	CH_3OH (40)[d]	TPMA	84.62	51.92	24.04	0.93	0.62	4.3
22	0.5[f]	CD_3OD (40)[d]	TPMA	81.52	54.97	22.52 (0)	0.82	0.71	2.1

[a] Conditions: [V-601] = 11.7 mg (0.050 mmol) in 0.7 mL of C_6D_6, 8 h at 75°C. [b] Ratio of the two C*H*$_3$C resonances (see SI) hence equivalent to the molar ratio of radicals leading to each product. [c] Average and standard deviation. [d] CH_3OH or CD_3OD (0.16 mL, 4 mmol). [e] CuBr (7.3 mg, 0.051 mmol), Cu^0 (13 mg, 0.204 mmol) and Me_6TREN (24 µL, 20.3 mg, 0.088 mmol). [f] CuBr (7.3 mg, 0.051 mmol), Cu^0 (13 mg, 0.204 mmol) and TPMA (25.6 mg, 0.088 mmol).

As found for the experiments in CD_3CN, the Disp/Comb ratio remained essentially invariant upon addition of methanol when no copper was present (Table 3, entries 15-16). A barely significant increase of this ratio in the presence of a copper complex and in the absence of proton donor (0.75±0.03 for CuBr/Cu^0/Me_6TREN, entry 17; 0.76±0.01 for CuBr/Cu^0/TPMA, entry 18), similar to the behavior in CD_3CN, suggests again a possible CRT contribution in favor of disproportionation. The smaller Disp/Comb ratio increase upon addition of Cu^I/L in C_6D_6 may be at least in part related to the greater solvent microviscosity, reducing the fraction of diffused radicals. However, according to the literature,[38] nearly 50% of the (COOMe)$Me_2C^{\bullet}$ radicals produced from V-601 in C_6D_6 should diffuse out of the cage prior to terminating. Nevertheless, the Disp/Comb increase upon addition of Cu^I/L in C_6D_6 (by only 0.03 units, *cf.* entries 14 and 17-18, Table 3) is less than even 50% of the corresponding increase in CD_3CN (by 0.14 units, *cf.* entries 1 and 4-5, Table 1). This suggests that the impact of CRT may be smaller in C_6D_6 than in CD_3CN. The percent of oligomers for all control experiments (entries 14-18) calculated from equation 2 (Scheme 6) where %Disp = %R-H, since there cannot be any RRT, averages to 20.1±0.4. The subsequent application of equation 3 yields an average value of (0.0±0.4) for the %RRT of these control experiments.

The analysis of the product distributions for the experiments run with the simultaneous addition of copper and proton donor (entries 19-22) followed the same procedure described in the previous section and the %RRT was calculated according to equation 3 (Scheme 6). In these experiments, the product distribution was significantly skewed in favor of R-H, much more than for the experiments run in CD_3CN and significantly outside of the error bar, especially when CH_3OH was used. Lower % RRT values for CD_3OD are consistent with the presence of a deuterium isotope effect. However, the amount of putative R-D produced by RRT with CD_3OD was still insufficient

to be directly detected in the ^{1}H NMR spectrum. The results suggest that the impact of RRT, albeit small, is greater in C_6D_6 than in CD_3CN, consistent with the greater proton donor strength of methanol in benzene as a consequence of the weaker proton acceptor power of this solvent. The impact of RRT appears consistently greater for the Me_6TREN system (12.2% with MeOH, entry 19; 7.4% with CD_3OD, entry 20) than for the TPMA system (4.3% with MeOH, entry 21; 2.1% with CD_3OD, entry 22), which parallels the trend of the same two complexes in CD_3CN when using CH_3OH and CD_3OD (Table 1). On the other hand, an even greater impact of RRT is observed for the TPMA system when using $Et_3NH^+PF_6^-$ in MeCN (*cf.* entries 9 and 3 in Table 1). Unfortunately, $Et_3NH^+PF_6^-$ cannot be used as proton donor in C_6D_6 due to solubility issues.

b. Terminations from MBiB.

The activation of MBiB by Cu^I/L (L = Me_6TREN, TPMA) to produce the carbomethoxyisopropyl radical requires one equivalent of metal complex, with concomitant formation of Br-Cu^{II}/L (see Scheme 5). To ensure efficient trapping of the generated radicals, the investigations in CD_3CN made use of 2 equivalents of the $[Cu^I(MeCN)_4]^+$ complex per MBiB. For the experiments with the Cu^IBr/Cu^0/L activator in C_6D_6, the excess Cu^0 converts the Br-Cu^{II}/L product back to Cu^I/L, thus the initial Cu^I/MBiB ratio was set to 1. The experiments run with $[Cu^I(MeCN)_4]^+$/Me_6TREN in CD_3CN revealed the presence of a competing MBiB reactivity with the ligand, generating ammonium cation, which was confirmed by control experiments (see SI, Figure S3). However, this side process was minor. The distribution of the radical termination products was calculated without consideration of the resonances resulting from this side reactivity. No significant side-product formation, on the other hand, was observed for the experiments carried out with activation by $[Cu^I(MeCN)_4]^+$/TPMA in CD_3CN and for those with Cu^IBr/Cu^0/L in C_6D_6

for both ligands. All results are collected in Table 4. The strongly activating Cu^{I}/L systems generated the radical from MBiB much faster than the thermal V-601 decomposition at the same temperatures. This is especially true for the more powerful Cu^{I}/Me_6TREN activator, leading to full MBiB consumption within 4 h in both solvents, whereas traces of residual MBiB remained in CD_3CN and conversions around 95% in C_6D_6 were obtained after 4 h when using Cu^{I}/TPMA.

Table 4. Product distribution from the termination of carbomethoxyisopropyl radicals generated by atom transfer activation of MBiB under various conditions.[a]

Entry	Solv.	Additive (equiv per R)	L	MBiB conv.	R-R	R-H (%D)	$2\frac{R-H}{R-R}$ [b]	MMA
23	CD_3CN[c]	-	Me_6TREN	100	49.26	25.37	1.03	11.67
24	CD_3CN[c]	CH_3OH (100)[d]	Me_6TREN	100	49.50	25.25	1.02	12.33
25	CD_3CN[c]	CD_3OD (100)[d]	Me_6TREN	100	48.37	25.81 (0)	1.07	10.50
26	CD_3CN[c]	$Et_3NH^+BF_4^-$ (1)[e]	Me_6TREN	100	48.54	25.73	1.06	10.92
27	CD_3CN[c]	$Et_3NH^+BF_4^-$ (20)[e]	Me_6TREN	100	48.51	25.75	1.06	7.94
28	C_6D_6[f]	-	Me_6TREN	100	51.72	24.14	0.93	3.52
29	C_6D_6[f]	CH_3OH (100)[g]	Me_6TREN	100	51.18	24.41	0.95	7.52
30	C_6D_6[f]	CD_3OD (100)[g]	Me_6TREN	100	49.95	25.02 (0)	1.00	4.80
31	CD_3CN[h]	-	TPMA	99.9	46.20	26.90	1.16	9.15
32	CD_3CN[h]	CH_3OH (100)[d]	TPMA	>99.9	46.64	26.68	1.14	9.70
33	CD_3CN[h]	CD_3OD (100)[d]	TPMA	>99.9	47.17	26.42 (0)	1.12	9.10
34	CD_3CN[h]	$Et_3NH^+BF_4^-$ (1)[e]	TPMA	>99.9	46.14	26.93	1.17	8.21
35	CD_3CN[h]	$Et_3NH^+BF_4^-$ (20)[e]	TPMA	>99.9	46.83	26.58	1.14	10.40
36	C_6D_6[i]	-	TPMA	96.18	52.19	23.90	0.92	3.50
37	C_6D_6[i]	CH_3OH (100)[g]	TPMA	95.25	49.04	25.48	1.04	4.66
38	C_6D_6[i]	CD_3OD (100)[f]	TPMA	95.24	49.37	25.31 (0)	1.02	4.99

[a] All experiments were carried out in thoroughly dehydrated solvents (see SI, section S1). [b] Ratio of the two C*H*$_3$C resonances (see SI) hence equivalent to the molar ratio of radicals leading to each product. [c] Conditions in CD_3CN: [MBiB] = 4.0 mg (0.022 mmol), $[Cu(MeCN)_4]BF_4$ (13.8 mg, 0.044 mmol) and Me_6TREN (24 µL, 20.3 mg, 0.088 mmol) in 0.7 mL of solvent, 4 h at 80°C. [d] CH_3OH or CD_3OD (89 µL, 2.2 mmol). [e] $Et_3NH^+BF_4^-$ (4.2 mg, 0.022 mmol, 1 eq.) or (83.2 mg, 0.44 mmol, 20 eq.). [f] Conditions in C_6D_6: [MBiB] = 9.2 mg (0.051 mmol), CuBr (7.3 mg, 0.051 mmol), Cu^0 (13 mg, 0.204 mmol) and Me_6TREN (24 µL, 20.3 mg, 0.088 mmol) in 0.7 mL of solvent, 4 h at 70°C. [g] CH_3OH or CD_3OD (0.21 mL, 5.1 mmol). [h] Conditions in CD_3CN: [MBiB] = 4.0 mg (0.022 mmol), $[Cu(MeCN)_4]BF_4$ (13.8 mg, 0.044 mmol) and TPMA (25.6 mg, 0.088 mmol) in 0.7 mL of solvent, 4 h at 80°C. [i] Conditions in C_6D_6: [MBiB] = 9.2 mg (0.051 mmol), CuBr (7.3 mg, 0.051 mmol), Cu^0 (13 mg, 0.204 mmol) and TPMA (25.6 mg, 0.088 mmol) in 0.7 mL of solvent, 4 h at 70°C.

The most relevant difference with respect to the equivalent radical generation from V-601 is the lower oligomer amount and correspondingly greater amount of MMA, as illustrated by a comparison of the ^{1}H NMR spectra in the vinyl proton region (Figure 1). The oligomer vinyl resonances are undetectable for all experiments run with Cu^I/Me_3TREN in CD_3CN, barely detectable for those run with Cu^I/TPMA in CD_3CN, while greater amounts (though still much smaller relative to the thermal activation of V-601) are visible for the experiments run with Cu^I/L in C_6D_6. For the latter, the oligomer/MMA ratio is slightly greater when L = TPMA. These trends can be rationalized by the much faster radical generation by atom transfer from MBiB relative to the thermal activation of V-601, and by the known rate constant trends for the MBiB/Cu^I/L atom transfer activation: TPMA < Me_6TREN and C_6D_6 < CD_3CN.[15, 17, 45] Indeed, an instantaneously greater radical concentration increases the termination rate ($k_t[R^\bullet]^2$) over the propagation rate ($k_p[R^\bullet][MMA]$), thus the MMA/oligomer ratio increases as the activation rate increases. This proposition is confirmed by the PREDICI simulations (*vide infra*).

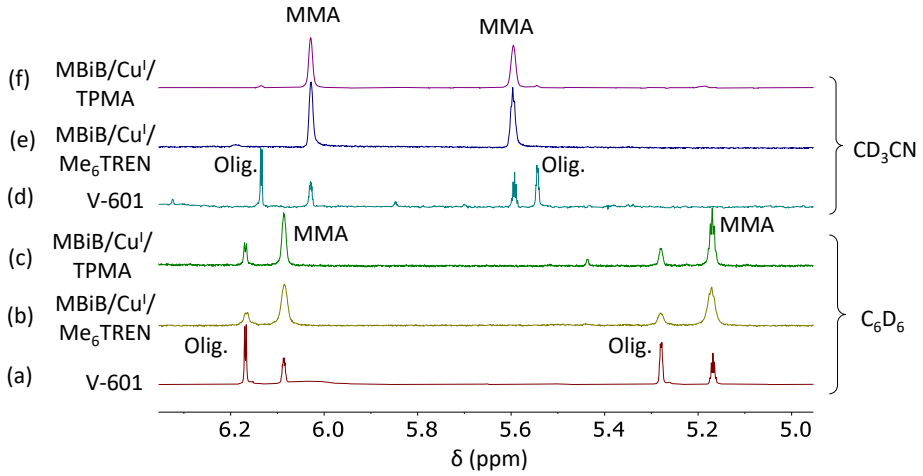

Figure 1. Expansion of the ^{1}H NMR spectrum in the sp^2 C-H resonance region for: (a) entry 14 (Table 3); (b) entry 28 (Table 4); (c) entry 36 (Table 4); (d) entry 1 (Table 1); (e) entry 23 (Table 4); (f) entry 31 (Table 4).

In terms of the R-R/R-H product distribution, let us first compare the results obtained in CD_3N, in the absence of proton donor additives, for the MBiB/Cu^I/L activation (L = Me_6TREN, entry 23; L = TPMA, entry 31) with those of the thermal V-601 activation (Table 1, entries 4 and 5, respectively). Since there cannot be any RRT in the absence of proton donors, the $2\frac{R-H}{R-R}$ ratio also corresponds to the Disp/Comb ratio (Scheme 6, equations 1 and 3). Making abstraction of the fate of the unsaturated disproportionation product (MMA *vs.* oligomers), the product distributions are identical within experimental error, independently of the radical source, for each ligand system. This may have been expected, because the two activation coproducts (N_2 from V-601 and Br-Cu^{II}/L from MBiB) do not interfere, neither with RT nor with CRT. It has to be pointed out, however, that the radicals are generated in quite different environments: in a {radical,N_2,radical} cage by thermal V-601 activation and in a {radical,BrCu^{II}/L} cage by atom transfer activation. In the former case, both caged and diffused radicals may terminate by RT, whereas CRT may only occur for the diffused radicals. In the latter case, on the other hand, there is no termination within the radical cage; all terminations may only take place after radical diffusion. Evidently, this difference does not significantly affect the outcome of the product distribution from the two different types of activation in CD_3CN, probably because the fraction of diffused radicals in this solvent is extensive. The different product distributions for the experiments run in the presence of Cu^I/Me_3TREN and Cu^I/TPMA, as already pointed out above, may be attributed to a greater efficiency of the latter in CRT, in favor of Disp.

Next, we can compare the termination results for the two different types of radical generation in C_6D_6, again in the absence of proton donors (entry 28 of Table 4 *vs.* entry 17 of Table 3 for Cu^I/Me_6TREN, entry 36 of Table 4 *vs.* entry 18 of Table 3 for Cu^I/TPMA). In this case, the Disp/Comb ratio is very much dependent on the activation method, whereas it is not significantly

affected by the nature of L. There is more disproportionation when the radical is obtained by MBiB/Cu^I/L activation (Disp/Comb = 0.93 and 0.92 for L = Me_6TREN and TPMA, entries 28 and 36 in Table 4, respectively) than when it is obtained by thermal V-601 activation in the presence of Cu^I/L (0.75±0.3 and 0.76±0.1 for L = Me_6TREN and TPMA, entries 17 and 18 in Table 3, respectively). As already argued above, the fraction of diffused radicals from the V-601 activation should in principle be smaller in C_6D_6 (estimated as 53% at 60 °C and 55% at 80 °C)[38] than in CD_3CN because of the microviscosity difference (Table 2). This would imply that the CRT/RT ratio should be smaller in the V-601 activation experiments, since the caged radicals can only terminate by RT. A greater Disp/Comb ratio for the diffused radicals hints to a possible contribution of CRT, if indeed CRT favors Disp. However, as shown above, the presence of Cu^I/L increases the Disp/Comb ratio only by *ca.* 0.03 units for the V-601 activation in C_6D_6, extrapolating to a maximum effect of 0.06 units for the diffused radicals if the fraction of the latter is ca. 50%.[38] On the other hand, the Disp/Comb ratio is ca. 0.20 units greater for the radicals generated from the MBiB atom transfer activation. Therefore, the major difference of this increase must be a greater Disp/Comb ratio for the diffused radicals relative to the caged ones. Indeed, Yamago *et al.* reported a slightly greater Disp/Comb ratio for the termination of the diffused radicals (at 80 °C: $Disp_{(cage)}/Comb_{(cage)}$ = 43:57 = 0.754; $Disp_{(dif)}/Comb_{(dif)}$ = 45:55 = 0.818; at 60 °C: $Disp_{(cage)}/Comb_{(cage)}$ = 44:56 = 0.786; $Disp_{(dif)}/Comb_{(dif)}$ = 46:54 = 0.852). Our measured ratios for the experiments in entries 28 and 36 (Table 4), in which all terminations occur on the diffused radicals, are higher still, the difference being possibly contributed by CRT. To summarize the effect of CRT (presence of Cu^I/L, absence of proton donors) in CD_3CN and C_6D_6, the former solvent yields Disp/Comb ratios that depend on the presence of Cu^I/L (TPMA > Me_6TREN) but not on the radical generation method (V-601 or MBiB), because both methods yield a total or

extensive fraction of terminations on diffused radicals and the CRT activity is greater in this solvent. The latter solvent yields Disp/Comb ratios that depend more strongly on the radical generation method and very little on the presence of Cu^{I}/L, because there is a greater fraction of caged radical terminations, which yield a significantly lower Disp/Comb ratio, and the CRT activity is lower than in CD_3CN but still sufficient to provide a contribution to the Disp/Comb ratio of the diffused radicals.

Turning now to the terminations of the carbomethoxyisopropyl radicals generated by the MBiB/Cu^{I}/L activation in the presence of proton donors, there is again a difference with respect to the related experiments where the same radicals are generated by thermal V-601 activations in the presence of Cu^{I}/L. Whereas, for the radicals generated from V-601, the presence of the proton donor gave small but significant changes in the R-R and R-H product distributions, both in CD_3CN (Table 1) and in C_6D_6 (Table 3), in agreement with a small impact of RRT, the product distributions and the Disp/Comb ratios are not significantly altered by the proton donor for the MBiB/Cu^{I}/L activation, particularly in CD_3CN, including in the presence of the more acidic $Et_3NH^{+}BF_4^{-}$ (see Table 4). For the MBiB/Cu^{I}/Me_6TREN activations (entries 23-27), the average R-R and R-H fractions are 48.8±0.4% and 25.6±0.2%, respectively, and the average $2\frac{R-H}{R-R}$ ratio is 1.048±0.015. For the MBiB/Cu^{I}/TPMA activations (entries 31-35), the same averages are 46.6±0.3%, 26.70±0.14% and 1.146±0.013, respectively. The invariance of these parameters signals the insignificant impact of RRT. In C_6D_6, on the other hand, the presence of CH_3OH or CD_3OD slightly increases the %R-R, decreases the %R-H and increases the $2\frac{R-H}{R-R}$ ratio (see Table 4, entries 29-30 *vs.* 28 for L = Me_6TREN and 37-38 *vs.* 36 for L = TPMA). Once again, there is no visible D incorporation in the saturated product (R-D).

A lower impact of RRT when the radicals are generated by atom transfer activation may again be rationalized on the basis of the rate of radical generation, which affects the radical concentration. As shown in Scheme 7, while the RT and CRT rate laws are both second order in radical, the RRT rate law is only first order in radical. Thus, an increased radical concentration increases the RT and CRT rates to a much greater extent than the RRT rate, whereas it has no effect on the RT/CRT ratio, provided the Cu^{I}/L concentration is unchanged (as is the case in our experiments). To summarize the effect of proton donors on the carbomethoxyisopropyl radical termination in the presence of Cu^{I}/L, the RRT phenomenon has a relatively low impact and is detectable only for the slower radical generation by thermal activation of V-601, whereas it is undetectable (in CD_3CN) or barely detectable (in C_6D_6) for the faster radical generation by atom transfer from MBiB.

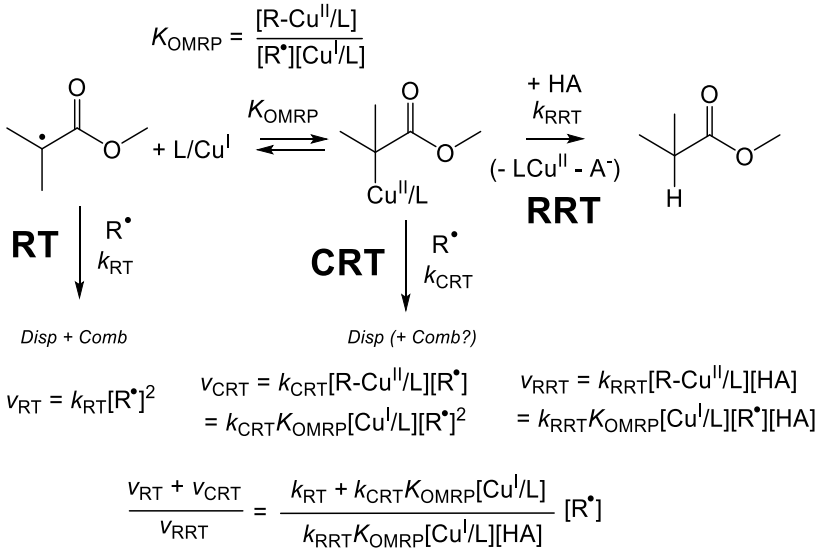

Scheme 7. Rates of different competing termination processes for the carbomethoxyisopropyl radical.

A final MBiB decomposition experiment was carried out in CD_3CN with the much poorer Cu^I/bpy activator under similar conditions. Being only a bidentate ligand, a double bpy/$[Cu(MeCN)_4]^+$ ratio was used relative to that used with the tetradentate Me_6TREN or TPMA ligands. The equilibrium constant for the ATRP activation step (K_{ATRP}, Scheme 1) of the related ethyl bromoisobutyrate in acetonitrile at 22°C is $3.8 \cdot 10^4$ times greater for the Cu^I/Me_6TREN activator than for Cu^I/bpy.[13] Indeed, MBiB was not completely consumed after 4 h at 80°C, see results in Table 5. The Disp/Comb ratio obtained for the experiments without proton donor (entry 39) and with 100 equiv of methanol (entry 40) are essentially identical and very close to those obtained with the Cu^I/Me_6TREN activator. In this case, the amount of MMA is barely detectable, consistent with the much slower radical production and thus lower steady-state radical concentration, which favors the oligomerization process. The sp^2 C-H resonance of the oligomer chain ends is also barely detectable, because the oligomers obtained with a slower radical production can grow to greater degrees of polymerization. By dividing the monomer amount in the oligomers (from the R-H and MMA amounts according to equation 2 of Scheme 3, given the absence of RRT, hence % Disp = % R-H) by the number of unsaturated oligomer chains (from the chain-end sp^2 C-H resonance intensity) yields values in the 35-50 range, whereas the corresponding ratios obtained from the V-601 decomposition experiments are on the average 20±3 (experiments in CD_3CN) and 12.6±0.6 (experiments in C_6D_6). These numbers do not correspond to the average degrees of polymerization because they do not consider the saturated oligomer chains produced by combination. However, this comparison provides a consistent picture of the aptitude of the produced MMA to undergo oligomerization under different conditions: the MMA amount decreases while the oligomer degree of polymerization correspondingly increases as the

rate of radical production decreases (MBiB/Cu^{I}/Me_6TREN > MBiB/Cu^{I}/TPMA > V-601 > MBiB/Cu^{I}/bpy).

Table 5. Product distribution from the termination of carbomethoxyisopropyl radicals generated by atom transfer activation of MBiB with the bpy ligand in CD_3CN.[a]

Entry	Solv.	Additive (equiv per R)	MBiB conv.	R-R	R-H (%D)	$2\frac{R-H}{R-R}$ [b]	MMA
39	CD_3CN	-	72.0	45.9	27.0	1.18	0.28
40	CD_3CN	CH_3OH (100)[c]	65.9	46.0	27.0	1.18	0.37

[a] Conditions: [MBiB] = 4.0 mg (0.022 mmol), $[Cu(MeCN)_4]BF_4$ (13.8 mg, 0.044 mmol) and bpy (27.5 mg, 0.176 mmol) in 0.7 mL of thoroughly dried CD_3CN, 4 h at 80°C. [b] Ratio of the two C*H*$_3$C resonances (see SI) hence equivalent to the molar ratio of radicals leading to each product. [c] CH_3OH (89 µL, 2.2 mmol).

c. PREDICI simulations

Kinetic simulations were performed using the package PREDICI® (v11.0) to determine whether the observed slight increase in the disproportionation products of the carbomethoxyisopropyl radical termination, when the latter is generated from V-601 in the presence of Cu^{I}/Me_6TREN, is compatible with realistic kinetic values.[46] Secondly, the simulations also assessed whether the observed amounts of MMA in the different experiments are compatible with the corresponding radical fluxes.

In the kinetic model used for the simulations (Scheme 8), radicals are reversibly deactivated by Cu^{I}/L centers (OMRP equilibria) and terminate *via* interaction of the organometallic intermediate species with a second radical. This model was also previously used for the catalyzed termination of the carbomethoxyethyl radical (a poly(methyl acrylate) radical analog), generated by atom transfer activation of MBP, using electrochemically-derived ATRP-OMRP-CRT rate constants.[21, 47] In those studies, the carbomethoxyisopropyl radical was found to bind to Cu^{I}/TPMA

too weakly to retrieve meaningful OMRP-CRT parameters from the experiments. Thus, the current modelling effort to recreate experimental termination distributions was built on the basis of the following considerations and assumptions: (*i*) the organometallic deactivation rate constants ($k_{d,RCu,OMRP}$ and $k_{d,PCu,OMRP}$) of the carbomethoxyisopropyl and oligo(methyl methacylate) radicals should be lower than an estimated value of 10^6 M^{-1} s^{-1}, which is based on the lack of detection by the standard electrochemical protocol; (*ii*) the organometallic equilibria ($K_{RCu,OMRP}$, $K_{PCu,OMRP}$), defined as the ratio of radical activation over deactivation) for the carbomethoxyisopropyl and oligo(methyl methacylate) radicals are expected to favor the unbound radical form much more (i.e. ~10^5 greater was used) than that of the carbomethoxyethyl radical with the same L/Cu species; (*iii*) the CRT rate constants ($k_{CRT,RR}$ and $k_{CRT,PP}$) are assumed to be similar to that of the carbomethoxyethyl radicals. These considerations are built on the hypothesis that the greater difficulty for the carbomethoxyisopropyl and polymethacrylate radicals to undergo CRT, relative to carbomethoxyethyl and polyacrylate radicals, is linked to their underlying lower ability of the tertiary radicals to bind to the Cu centers (OMRP equilibria), rather than to an increased barrier of the final product-releasing step from the organometallic intermediates. The experimental product distributions obtained from the termination of the carbomethoxyisopropyl radicals generated from V-601 in the absence and presence of Cu^I/Me_6TREN (Table 1, Entries 1 and 4, respectively) were thus modelled using these criteria and scaling from the known OMRP-CRT parameters of the carbomethoxyethyl radical.[21]

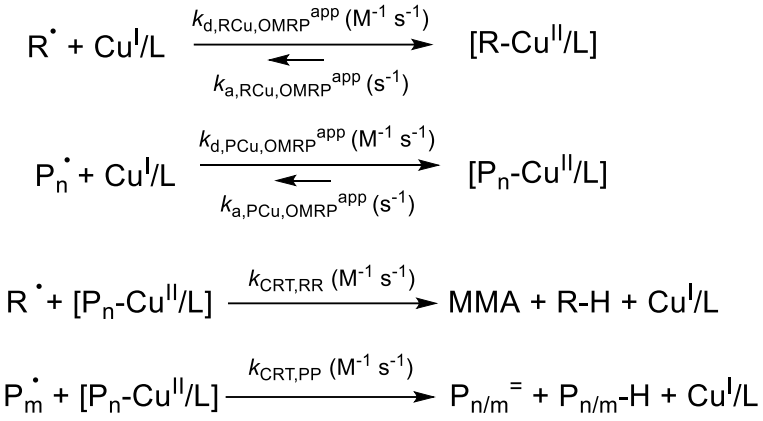

Scheme 8. Kinetic model used for the PREDICI simulations of the termination products from the V-601-generated carbomethoxyisopropyl (R) radicals in the presence of a Cu^I/L termination catalyst. $P_m^•$ and $P_n^•$ indicate oligo(methyl methacrylate) radicals

The kinetic parameters found to best fit the experimental results are collected in Table 6. The assumptions made to fix the addition, propagation and termination rate constants of the initiating and oligomeric radicals are justified in the Supporting Information (section S5). The OMRP activation, deactivation, and CRT rate constants were then manually scaled to reproduce the experimental product distribution, as detailed below (Table 7). First, apparent k_t values for combination and disproportionation ($k_{t,Rcomb}$ and $k_{t,Rdisp}$) were selected to mimic the combination-disproportionation product distribution resulting from the Cu-free control experiment of V-601 in CD_3CN at 80 ºC (Table 1, Entry 1), see Table 7, P1. Then, these parameters were incorporated into the PREDICI simulation of the product distribution of Table 1, Entry 4, in the presence of Cu^I/Me_6TREN (Table 7, P2).

Table 6. PREDICI-simulation model reactions and rate constants for the thermal decomposition of V-601 in MeCN at 80 °C in the presence of Cu^{I}/L.[a]

Reactions	Reactant 1	Reactant 2	Product 1	Product 2	Product 3	k^{b}	*value*	Reference
Thermal Decomposition	V-601		R•	R•		k_{td} (s^{-1})	1.65×10^{-4}	[c]
Radical Addition	R•	M	P_1•			$k_{add,R•}$	1.54×10^{4}	[48]
	R•	$P^{=}$	P_{n+1}•			$k_{add,R•P=}$	1.54×10^{4}	
Propagation	P_n•	M	P_{n+1}•			$k_{p,P•}$	1.54×10^{3}	[d]
	P_n•	$P_s^{=}$	P_{n+s}•			$k_{p,P•P=}$	1.54×10^{3}	
OMRP Activation	R-Cu^{II}/L		R•	Cu^{I}/L		$k_{a,RCu,OMRP}$ (s^{-1})	3.9	[21, e]
	P_n-Cu^{II}/L		P_n•	Cu^{I}/L		$k_{a,PCu,OMRP}$ (s^{-1})	10	
OMRP Deactivation	R•	Cu^{I}/L	R-Cu^{II}/L			$k_{d,RCu,OMRP}$	2.5×10^{2}	[21, e]
	P_n•	Cu^{I}/L	P_n-Cu^{II}/L			$k_{d,PCu,OMRP}$	1.7×10^{2}	
Combination Termination	R•	R•	R-R			$k_{t,Rcomb}$	4.98×10^{8}	[f,g]
	R•	P_n•	P_n-R			$k_{t,cross,comb}$	2.74×10^{8}	
	P_n•	P_s•	P_n-P_s			$k_{t,Pcomb}$	4.98×10^{7}	
Disproportionation Termination	R•	R•	R-H	$R^{=}$		$k_{t,Rdisp}$	5.02×10^{8}	[f]
	P_n•	P_n•	P_n-H	$P_n^{=}$		$k_{t,Pdisp}$	5.02×10^{7}	
Catalytic Radical Termination	R-Cu^{II}/L	R•	R-H	$R^{=}$	Cu^{I}/L	$k_{CRT,RR}$	9.0×10^{6}	[21,e]
	P_n-Cu^{II}/L	P_s•	$P_{n/s}$-H	$P_{n/s}^{=}$	Cu^{I}/L	$k_{CRT,PP}$	5.0×10^{6}	

[a] R• = carbomethoxyisopropyl radical, Me_2C•(COOMe); P_n•, P_s• = oligo(methyl methacrylate) radicals. [b] Unless otherwise specified, rate constants are in M^{-1} s^{-1}; the set of given rate constant values recreate the experimental termination product distributions under realistic kinetic regimes. [c] From the V-601 chemical supplier, Wako Chemicals, for 80 ºC. [d] Scaled from radical addition by a factor of 10. [e] Oligomer analog scaled from small-molecule by the same factor as between methyl 2-bromopropionate (MBP) and poly(methyl acrylate)-based macroinitiator (PMA-Br). [f] Sum of combination and disproportionation typical for small molecule radical equal to 10^9 and for oligomeric radical equal 10^8, based on the product distribution of Cu-free V-601 decomposition control experiment (Entry 1, Table 1) in CD_3CN. [g] This work.

Table 7. PREDICI-simulated product distributions for the termination products of the carbomethoxyisopropyl radicals generated from V-601 at 80 °C as a function of the OMRP-CRT rate constants ($k_{a,OMRP}$, $k_{d,OMRP}$, k_{CRT}) and thermal decomposition (k_{td}).[a]

Index	$k_{a,OMRP}$	$k_{d,OMRP}$	k_{CRT}	k_{td}	%R-R	%R-H	%MMA
(a) In the absence of Cu^{I}/TREN							
P1[b]	-	-	-	1.65×10^{-4}	49.80	25.10	0.68
Experimental (Table 1, Entry 1)					49.8±0.4	25.1±0.2	0.8±0.1
(b) In the presence of Cu^{I}/TREN (optimized)							
P2[b]	3.9	2.5×10^{2}	9.00×10^{6}	1.65×10^{-4}	48.20	25.90	0.72
Experimental (Table 1, Entry 4)					48.2±1.4	25.9±0.7	0.8±0.1
(c) In the presence of Cu^{I}/TREN (rate constant variations)[c]							
P3	÷100	-	-	-	34.22	32.89	1.84
P4	÷10	-	-	-	41.52	29.24	0.97
P5	×10	-	-	-	49.62	25.19	0.67
P6	×100	-	-	-	49.78	25.11	0.67
P7	-	÷100	-	-	49.78	25.11	0.67
P8	-	÷10	-	-	49.64	25.18	0.68
P9	-	×10	-	-	37.30	31.35	1.05
P10	-	×100	-	-	11.16	44.42	3.37
P11	-	-	÷100	-	49.78	25.11	0.67
P12	-	-	÷10	-	49.62	25.19	0.68
P13	-	-	×10	-	41.52	29.24	0.96
P14	-	-	×100	-	34.23	32.89	1.83
P15	-	-	-	×10	48.46	25.77	2.54
P16	-	-	-	×100	48.90	25.55	10.7
P17	-	-	-	×1000	49.34	25.33	18.7
P18	-	-	-	×10,000	49.61	25.20	22.7
P19	-	-	-	×100,000	49.73	25.13	24.3

[a] Conditions: V-601 = 0.022 mmol, $[Cu^{I}/L]^{+}$ = 0.044 mmol, V = 0.7 mL, t = 8 h, T = 80 ºC, V-601 conversion = 99.1%. [b] Other constants as shown in Table 6. [c] Rate constants are indicated as changes relative to the optimized value of P2. All rate constants of the same type, *i.e.* for small molecule and oligomer, are scaled equally.

Ranges of $k_{a,OMRP}$, $k_{d,OMRP}$, and k_{CRT} rate constants were explored to probe their influence on the termination product distribution (Table 7, P3-P14). Scaling up the OMRP activation rate constants (R-Cu^{II}/L and P_n-Cu^{II}/L homolytic bond cleavage) led to increasingly more coupled product,

asymptotically tending toward the P1 result, *via* a decrease of the organometallic species concentration and an increase of the free-radical forms (P5-P6). Likewise, scaling down the activation rate constants led to less coupling and more CRT as the radical adducts became less transient (P3-P4). Increasing the OMRP deactivation rate constants increased the organometallic species concentration and thus increased the disproportionation product (Table 7, P11-P12). Interestingly, the termination product distributions were not mirrored across equivalent changes in the OMRP equilibrium. For example, a 100-fold upscaling of the OMRP deactivation rate constant led to significantly lower combination (P10, %R-R = 11.16%) than a 100-fold downscaling of the OMRP activation rate constant (P3, %R-R = 34.22%), despite their equivalent effect on the K_{OMRP}. In other words, increasing the competitiveness of the deactivation reaction rate enhances the OMRP-CRT pathway more than an equivalent increase in merely stabilizing the radical adduct. Finally, an increase of the CRT rate constants, while maintaining the OMRP equilibrium unchanged, led to a substantial decrease of the Comb product as anticipated by increasing termination efficiency of organometallic complexes, and vice-versa. The effects of other OMRP-CRT parameter variations are discussed in the supporting information (section S6).

The effect of the radical flux on the impact of oligomerization was investigated by "artificially" increasing the rate constant of thermal decomposition (Table 7, P15-P19). Using the best estimate of k_{td} (Table 6) yields a percent of MMA in good agreement with the experimental result of Table 1 (Entry 4). A higher radical flux in the presence of the Cu^{I}/Me_6TREN termination catalyst leads to a smaller MMA oligomerization (Figure 2, top), as predicted above on the basis of the termination *vs.* addition/propagation/deactivation rate laws. All simulations began at the same %MMA (~25%) as predetermined by the rate constant, since no significant propagation occurs initially. Secondly, it was found that artificially increasing radical flux tended the system towards

Cu-free Comb/disp distributions, also as predicted above on the basis of the termination *vs.* addition/propagation/deactivation rate laws.

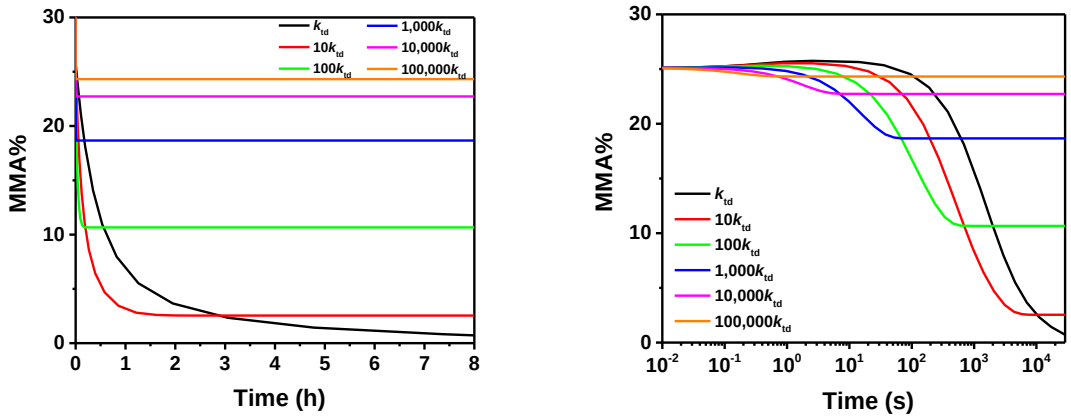

Figure 2. Percent of MMA present from the thermal decomposition of V-601 in the presence of Cu^{I}/Me_6TREN as a function of time (left – linear, right – logarithmic) and thermal decomposition rate constant (k_{td}).

Overall, the OMRP-CRT parameter analysis agrees with the anticipated effects on product distribution. Forcing the organometallic intermediates to more readily disassemble, to associate more slowly, or to terminate less efficiently leads to product distributions that approach that of the Cu-free experiment. The fraction of coupling product decreased and that of the disproportionation products correspondingly increased when the formation of the organometallic intermediates was enhanced.

d. DFT calculations

The aptitude of the carbomethoxyisopropyl radical to bind to Cu^{I} was probed for three different complexes, namely $[Cu(Me_6TREN)]^+$, $[Cu(TPMA)]^+$ and $[Cu(bpy)_2]^+$, in comparison with the results previously reported for the cyanoisopropyl analogue.[37] For the purpose of this comparison, the selected computational level (functional, basis sets and different corrections) was identical to

the previously used one (see details in the SI, section S4). Like the cyanoisopropyl radical, the carbomethoxyisopropyl radical benefits from resonance stabilization as shown in Scheme 9. Thus, it can bind either via the C atom as a tertiary alkyl ligand (**A**) or the O atom as an enolate (**B**), whereas the cyanoisopropyl radical can bind either via the C atom (**C**) or the N atom as a keteniminate (**D**). Both binding modes were probed in the calculations.

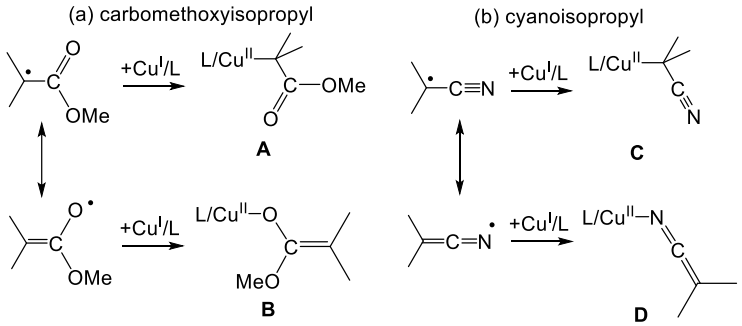

Scheme 9. Two different binding modes for the cyano- and carbomethoxyisopropyl radicals to Cu^{I}.

The energy results are summarized and compared with those of the related cyanoisopropyl bonding in Table 8. Views of the optimized geometries of the various carbomethoxyisopropyl-Cu^{II}/L adducts are shown in Figure 3. The first and most important observation is that the carbomethoxy radical always prefers to bind Cu^{II} as a tertiary alkyl (**A** in Scheme 9) rather than as an enolate. The cyano radical, on the other hand, was shown to form a more stable adduct as a keteniminate (**D**) rather than as a tertiary alkyl for all three ligand systems.[37] A second interesting observation is that the strongest Cu^{II}-C bonds for both carbomethoxy- and cyanoisopropyl radicals are obtained for the TPMA system. However, the Cu^{II}-N bond for the keteniminate adduct is marginally stronger for the Me_6TREN system. These trends can be rationalized on the basis of the greater steric impediments exerted by the bulkier Me_6TREN ligand to the establishment of the new Cu^{II}-X bond, which is felt to a greater extent for the more encumbered tertiary alkyl ligands. The Cu^{II}-

O bond in the enolate derivatives is also stronger in the TPMA system, probably again for steric reasons: the smaller Cu-O-C angle (137.3° for L = Me_6TREN and 130.9° for L = TPMA) and the two substituents on the β-C atom lead to a greater clash with the ligand electron density than the greater Cu-N=C angle (138.9° for L = Me_6TREN, 138.8° for L = TPMA and 140.1° for L = $(bpy)_2$)[37] and linear N=C=C moiety. Overall, the $[Cu(Me_6TREN)]^+$ fragment is more encumbered than the $[Cu(TPMA)]^+$ fragment and the carbomethoxy radical is more encumbered than the cyano radical (both as tertiary alkyl and in the heteroatom-bound form). It is also interesting to note that, for both radicals and in both binding modes, the bpy system leads to weaker binding. However, the carbomethoxy radical still leads to a slightly stabilized adduct in the C-bound form, whereas the cyano radical addition is endoergic, both in the C- and N-bound forms. Thus, although the DFT investigation predicts weak binding of the $^{\bullet}CMe_2COOMe$ radical, the organometallic Cu^{II} adduct does appear to form as a dormant species, particularly for the TPMA and Me_6TREN systems. A small interaction between tertiary methacrylate model radicals and copper complexes was also shown in recent electrochemical investigations of the 2-bromoisobutyrate (EBiB) activation by Cu^I/L systems.[21, 49]

Table 8. DFT-Estimated Gibbs' Free Energies ($\Delta G_{298.15,MeCN,1M}$ in kcal/mol) for the formation of $[Cu^{II}(CMe_2X)(L)_n]^+$ from $[Cu^I(L)_n]^+$ plus $Me_2XC^{\bullet}$ (X = COOMe, CN; L = Me_6TREN, TPMA, bpy).

	Carbomethoxyisopropyl system		Cyanoisopropyl system[a]	
L	$[(L)_nCu\text{-}CMe_2COMe]^+$	$[(L)_nCu\text{-}OC(OMe)=CMe_2]^+$	$[(L)_nCu\text{-}CMe_2CN]^+$	$[(L)_nCu\text{-}N=C=CMe_2]^+$
Me_6TREN, n = 1	-6.5	-2.8	-6.6	-12.9
TPMA, n = 1	-12.5	-11.9	-11.9	-12.6
bpy, n = 2	-1.8	+2.2[b]	+3.7[b]	+2.9

[a] Data from ref. [37]. [b] A stable adduct with a Cu^{II}-C bond could not be optimized. The optimized geometry corresponds to a van der Waals $[(L)Cu^I]^+\cdots$radical adduct.

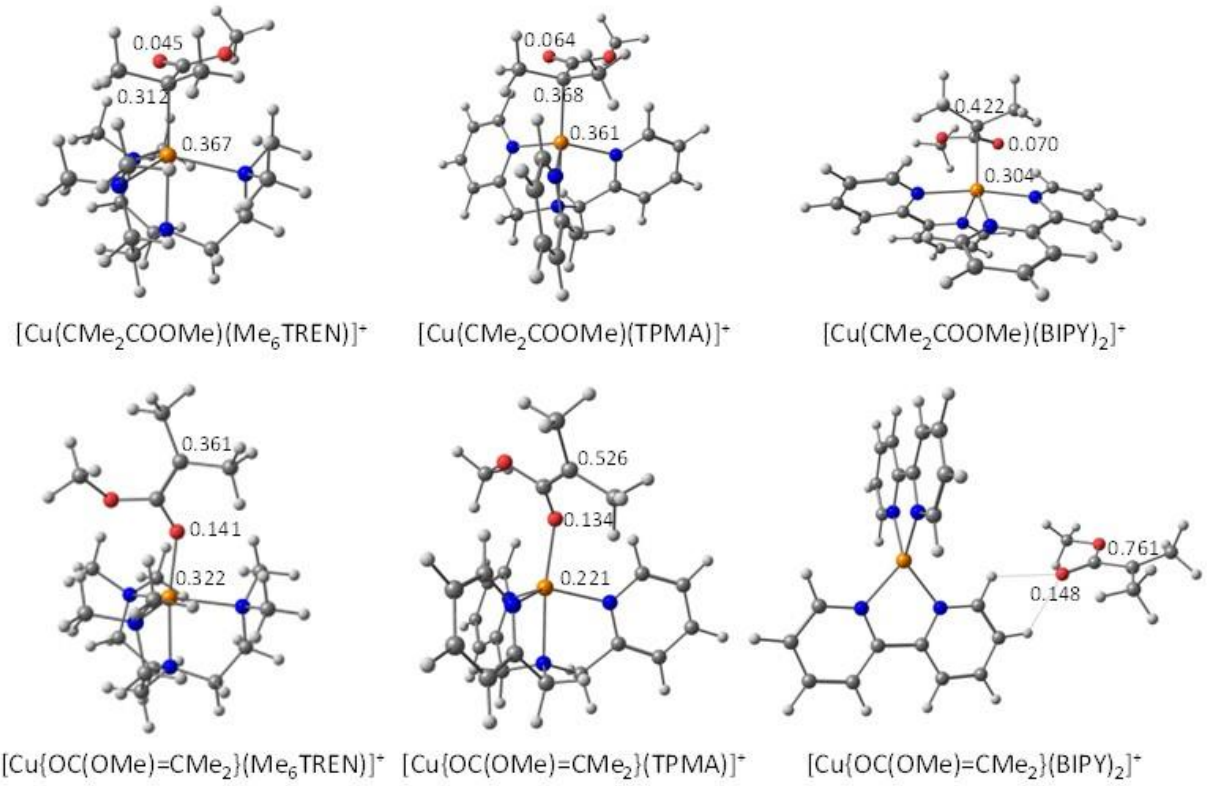

Figure 3. Views of the optimized $[Cu(Me_2CCOOMe)(L)]^+$ structures (L = Me_6TREN, TPMA, $(bpy)_2$) with the main Mulliken spin densities.

Comparison of $\Delta G_{298.15,MeCN,1M}$ for the $[(L)Cu\text{-}CMe_2X]^+$ (X = CN, COOMe) pairs (Table 8) shows slightly stronger binding of the carbomethoxy alkyl than for the cyano analogue (greater stabilization for the TPMA and bpy systems, approximately equal for the more encumbered Me_2TREN system). Consequently, the possible intervention of CRT and RRT might be expected for the carbomethoxyisopropyl radical and indeed both were observed, but only to a very small extent. It is useful to recall that the cyanoisopropyl radical leads to extensive RRT (in the order Me_2TREN > TPMA >> bpy), but no CRT.[37] This shows that a mechanism for quenching the organometallic intermediate by the action of a second radical is possible, though not very

favorable, only for •CMe_2COOMe, perhaps because the •CMe_2CN radical prefers to bind in the keteniminate form (**D** in Scheme 9). On the other hand, quenching by the action of a proton donor is favored for the cyano system and disfavored for the carbomethoxy system. This may again be related to the radical binding mode, because the Cu^{II}-N bond established by the cyano radical is more polar than the Cu^{II}-C bond established by the carbomethoxy radical. However, electronic control in the proton transfer reaction appears in contradiction with the calculated ground state charges (Table 9). Indeed, for each pair of complexes with the same L, the overall charge on the CMe_2X group is more negative for the less reactive carbomethoxy system and the charge localized on the proton-accepting C atom for the carbomethoxy system is much more negative than that localized on the C_γ atom for the cyano system, particularly for the more RRT-active Me_6TREN and TPMA systems. On the other hand, direct protonation at the C atom is sterically much less accessible for the C-bonded carbomethoxyisopropyl group than for the N-bonded cyanoisopropyl group, where this atom is in γ position relative to the metal center. This comparison hints a steric control. The negative charge on the keteniminate N atom, however, is high (see Table 9), thus N-protonation to yield a ketenimine (tautomer of the observed isobutyronitrile final product) appears more likely and seems also sterically accessible. The carbonyl γ O atom in the C-bonded carbomethoxyisopropyl group, which also bears a relatively high negative charge (Table 9), seems more accessible to protonation. This putative reaction would lead to an enol product that could subsequently tautomerize to methyl isobutyrate.

Table 9. Representative Mulliken charges in the $[Cu^{II}(CMe_2X)(L)_n]^+$ complexes.

	Carbomethoxyisopropyl system (C-bonded)	Cyanoisopropyl system[a] (N-bonded)

L	q_{Cu}	$q_{CMe2COOMe}$	q_{C}	$q_{O\gamma}$	q_{Cu}	q_{CMe2CN}	q_{N}	$q_{C\gamma}$
Me_6TREN, n = 1	0.280	-0.181	-0.452	-0.385	0.249	-0.170	-0.458	-0.176
TPMA, n = 1	0.382	-0.152	-0.446	-0.393	0.392	-0.090	-0.470	-0.147
bpy, n = 2	0.486	-0.144	-0.387	-0.397	0.486	-0.108	-0.460	-0.146

Conclusions

The termination of the carbomethoxyisopropyl radical, whether generated from V-601 or from MBiB, is not affected by the combined action of a Cu^I/L complex and a proton donor (MeOH, Et_3NH^+) in an RRT process, whereas the same additives have a profound effect on the RRT of the cyanoisopropyl radical generated from AIBN.[37] However, the presence of Cu^I/L introduces a small CRT contribution for the termination of the carbomethoxyisopropyl and oligo(methyl methacrylate) radicals, in the other Cu^I/TPMA > Cu^I/Me_6TREN > Cu^I/bpy (no evidence) and CD_3CN > C_6D_6, whereas no CRT was evident for the cyanoisopropyl radical. The DFT calculations suggest that these differences are related to the preferential C-binding of the carbomethoxyisopropyl radical, whereas the cyanoisopropyl radical prefers to bind in the keteniminate form via the N atom.

The small or no impact of CRT for the termination of these two tertiary $^{\bullet}CMe_2X$ radicals (X = COOMe, CN) is interesting when compared with the high propensity of the secondary acrylate radicals toward this catalyzed termination pathway,[26, 32] which was proven to require transit through an organometallic Cu^{II} intermediate.[20, 21] Experimental termination experiments and computations for systems involving acrylate radicals, analogous to those presented here, aiming at

a deeper understanding of the mechanism and limitations of the CRT and RRT processes, are currently in progress in our laboratories and will be reported in due course.

ASSOCIATED CONTENT

Supporting Information. Experimental procedures, method used for the determination of the relative amounts of termination products, results of the microviscosity determinations, additional considerations and results of the PREDICI simulations, computational details and results (20 pages).

AUTHOR INFORMATION

Corresponding Authors

* Krzysztof Matyjaszewski, km3b@andrew.cmu.edu.

* Rinaldo Poli, rinaldo.poli@lcc-toulouse.fr.

* Christophe Fliedel, christophe.fliedel@lcc-toulouse.fr

Author Contributions

The manuscript was written through contributions of all authors. All authors have given approval to the final version of the manuscript.

Funding Sources

National Science Foundation (USA), CHE 2000391; Centre National de la Recherche Scientifique (France), IRP LCC-CRP; Ministère de l'Enseignement Supérieur et de la Recherche Scientifique (France); French Embassy (Washington DC, USA), Chateaubriand fellowship.

ACKNOWLEDGMENT

Financial support from NSF (CHE 2000391), from CNRS (IRP LCC-CRP), from the Ministère de l'Enseignement Supérieur et de la Recherche Scientifique (Ph.D. fellowship to LT) and from the French Embassy in the USA (Chateaubriand fellowship to JS) is gratefully acknowledged. We thank Yannick Coppel and Christian Bijani (NMR service of the LCC-Toulouse) for the NMR-DOSY measurements.

ABBREVIATIONS

ATRP, Atom Transfer Radical Polymerization; bpy, 2,2'-bipyridine; CRT, Catalyzed Radical Termination; MBiB, methyl 2-bromoisobutyrate; Me_6TREN, tris[(2-dimethylamino)ethyl]amine; OMRP, Organometallic-Mediated Radical Polymerization; RRT, Reductive Radical Termination; TPMA, tris(2-pyridylmethyl)amine; V-601, dimethyl 2,2'-azobis(2-methylpropionate).

REFERENCES

1. Fischer, H. The Persistent Radical Effect: A Principle for Selective Radical Reactions and Living Radical Polymerizations. *Chem. Rev.* **2001,** 101 (12), 3581-3610.
2. Jenkins, A. D.; Jones, R. G.; Moad, G. Terminology for reversible-deactivation radical polymerization previously called "controlled" radical or "living" radical polymerization (IUPAC Recommendations 2010). *Pure Appl. Chem.* **2010,** 82 (2), 483-491 DOI: 10.1351/pac-rep-08-04-03.
3. Corrigan, N.; Jung, K.; Moad, G.; Hawker, C. J.; Matyjaszewski, K.; Boyer, C. Reversible-deactivation radical polymerization (Controlled/living radical polymerization): From discovery to materials design and applications. *Progr. Polym. Sci.* **2020,** 111, DOI: 10.1016/j.progpolymsci.2020.101311.
4. Matyjaszewski, K.; Xia, J. H. Atom transfer radical polymerization. *Chem. Rev.* **2001,** 101 (9), 2921-2990 DOI: 10.1021/cr940534g.
5. Kamigaito, M.; Ando, T.; Sawamoto, M. Metal-catalyzed living radical polymerization. *Chem. Rev.* **2001,** 101 (12), 3689-3745.
6. di Lena, F.; Matyjaszewski, K. Transition metal catalysts for controlled radical polymerization. *Progr. Polym. Sci.* **2010,** 35 (8), 959-1021.
7. Matyjaszewski, K. Atom Transfer Radical Polymerization (ATRP): Current Status and Future Perspectives. *Macromolecules* **2012,** 45 (10), 4015-4039 DOI: 10.1021/ma3001719.

8. Lorandi, F.; Fantin, M.; Matyjaszewski, K. Atom Transfer Radical Polymerization: A Mechanistic Perspective. *J. Am. Chem. Soc.* **2022,** 144 (34), 15413-15430 DOI: 10.1021/jacs.2c05364.
9. Fliedel, C.; Dagorne, S.; Le Roux, E. In *Comprehensive Coordination Chemistry III*; Constable, E. C., Parkin, G., Que Jr, L., Ed.; Elsevier: Oxford, 2021; pp 410-464.
10. Matyjaszewski, K.; Tsarevsky, N. V. Macromolecular Engineering by Atom Transfer Radical Polymerization. *J. Am. Chem. Soc.* **2014,** 136 (18), 6513-6533 DOI: 10.1021/ja408069v.
11. Yan, J. J.; Bockstaller, M. R.; Matyjaszewski, K. Brush-modified materials: Control of molecular architecture, assembly behavior, properties and applications. *Progr. Polym. Sci.* **2020,** 100, DOI: 10.1016/j.progpolymsci.2019.101180.
12. Baker, S. L.; Kaupbayeva, B.; Lathwal, S.; Das, S. R.; Russell, A. J.; Matyjaszewski, K. Atom Transfer Radical Polymerization for Biorelated Hybrid Materials. *Biomacromolecules* **2019,** 20 (12), 4272-4298 DOI: 10.1021/acs.biomac.9b01271.
13. Tang, W.; Kwak, Y.; Braunecker, W.; Tsarevsky, N. V.; Coote, M. L.; Matyjaszewski, K. Understanding atom transfer radical polymerization: Effect of ligand and initiator structures on the equilibrium constants. *J. Am. Chem. Soc.* **2008,** 130 (32), 10702-10713.
14. Braunecker, W. A.; Tsarevsky, N. V.; Gennaro, A.; Matyjaszewski, K. Thermodynamic Components of the Atom Transfer Radical Polymerization Equilibrium: Quantifying Solvent Effects. *Macromolecules* **2009,** 42 (17), 6348-6360 DOI: 10.1021/ma901094s.
15. Horn, M.; Matyjaszewski, K. Solvent Effects on the Activation Rate Constant in Atom Transfer Radical Polymerization. *Macromolecules* **2013,** 46 (9), 3350-3357 DOI: 10.1021/ma400565k.
16. Ribelli, T. G.; Fantin, M.; Daran, J.-C.; Augustine, K. F.; Poli, R.; Matyjaszewski, K. Synthesis and Characterization of the Most Active Copper-based ATRP Catalyst based on tris[(4-dimethylaminopyridyl)methyl]amine *J. Am. Chem. Soc.* **2018,** 140, 1525–1534 DOI: https://doi.org/10.1021/jacs.7b12180.
17. Ribelli, T. G.; Lorandi, F.; Fantin, M.; Matyjaszewski, K. Atom Transfer Radical Polymerization: Billion Times More Active Catalysts and New Initiation Systems. *Macromol. Rapid Comm.* **2019,** 40 (1), 1800616 DOI: 10.1002/marc.201800616.
18. Lorandi, F.; Matyjaszewski, K. Why Do We Need More Active ATRP Catalysts? *Isr. J. Chem.* **2020,** 60 (1-2), 108-123 DOI: 10.1002/ijch.201900079.
19. Enciso, A. E.; Lorandi, F.; Mehmood, A.; Fantin, M.; Szczepaniak, G.; Janesko, B. G.; Matyjaszewski, K. p-Substituted Tris(2-pyridylmethyl)amines as Ligands for Highly Active ATRP Catalysts: Facile Synthesis and Characterization. *Angew. Chem. Int. Ed.* **2020,** 59, 14910-14920 DOI: 10.1002/anie.202004724.
20. Ribelli, T. G.; Rahaman, S. M. W.; Daran, J.-C.; Krys, P.; Matyjaszewski, K.; Poli, R. Effect of Ligand Structure on the Cu^{II}-R OMRP Dormant Species and its Consequences for Catalytic Radical Termination in ATRP. *Macromolecules* **2016,** 49, 7749–7757 DOI: https://doi.org/10.1021/acs.macromol.6b01334.
21. Fantin, M.; Lorandi, F.; Ribelli, T. G.; Fliedel, C.; Thevenin, L.; Isse, A. A.; Poli, R.; Matyjaszewski, K. Impact of Organometallic Intermediates on Copper-Catalyzed Atom Transfer Radical Polymerization. *Macromolecules* **2019,** 52, 4079-4090 DOI: https://doi.org/10.1021/acs.macromol.9b00870.
22. Zerk, T. J.; Bernhardt, P. V. Organo-Copper(II) Complexes as Products of Radical Atom Transfer. *Inorg. Chem.* **2017,** 56 (10), 5784-5792 DOI: https://doi.org/10.1021/acs.inorgchem.7b00402.

23. Le Grognec, E.; Claverie, J.; Poli, R. Radical Polymerization of Styrene controlled by Half-Sandwich Mo(III)/Mo(IV) Couples: all Basic Mechanisms are Possible. *J. Am. Chem. Soc.* **2001,** 123, 9513-9524 DOI: https://doi.org/10.1021/ja010998d.
24. Poli, R. Relationship between one-electron transition metal reactivity and radical polymerization processes. *Angew. Chem. Int. Ed.* **2006,** 45, 5058–5070.
25. Schröder, K.; Konkolewicz, D.; Poli, R.; Matyjaszewski, K. Formation and Possible Reactions of an Organometallic Intermediate with Active Copper(I) Catalysts in an ATRP. *Organometallics* **2012,** 31, 7994-7999 DOI: https://doi.org/10.1021/om3006883.
26. Wang, Y.; Soerensen, N.; Zhong, M.; Schroeder, H.; Buback, M.; Matyjaszewski, K. Improving the "Livingness" of ATRP by Reducing Cu Catalyst Concentration. *Macromolecules* **2013,** 46 (3), 683-691 DOI: https://doi.org/10.1021/ma3024393.
27. Thevenin, L.; Fliedel, C.; Matyjaszewski, K.; Poli, R. Impact of catalyzed radical termination (CRT) and reductive radical termination (RRT) in metal-mediated radical polymerization processes. *Eur. J. Inorg. Chem.* **2019**, 4489–4499 DOI: https://doi.org/10.1002/ejic.201900901.
28. Cohen, H.; Meyerstein, D. Kinetics of Formation and Decomposition of the Methyl Copper(II) Complex in Aqueous-Solutions - a Pulse-Radiolysis Study. *Inorg. Chem.* **1986,** 25 (9), 1505-1506 DOI: https://doi.org/10.1021/ic00229a043.
29. Cohen, H.; Meyerstein, D. Kinetics of beta-hydroxyl elimination from $(H_2O)_mCu^{II}CH_2C(CH_3)_2OH^+$ in aqueous solution - a pulse radiolysis study. *J. Chem. Soc., Faraday Trans I* **1988,** 84, 4157-4160 DOI: https://doi.org/10.1039/f19888404157.
30. Ribelli, T. G.; Matyjaszewski, K.; Poli, R. The interaction of carbon-centered radicals with copper(I) and copper(II) complexes. *J. Coord. Chem.* **2018,** 71, 1641-1668 DOI: https://doi.org/10.1080/00958972.2018.1490416.
31. Nakamura, Y.; Ogihara, T.; Yamago, S. Mechanism of Cu(I)/Cu(0)-Mediated Reductive Coupling Reactions of Bromine-Terminated Polyacrylates, Polymethacrylates, and Polystyrene. *ACS Macro Lett.* **2016,** 5 (2), 248-252 DOI: 10.1021/acsmacrolett.5b00947.
32. Ribelli, T. G.; Augustine, K. F.; Fantin, M.; Krys, P.; Poli, R.; Matyjaszewski, K. Disproportionation or Combination? The Termination of Acrylate Radicals in ATRP. *Macromolecules* **2017,** 50, 7920–7929 DOI: https://doi.org/10.1021/acs.macromol.7b01552.
33. Nakamura, Y.; Yamago, S. Termination Mechanism in the Radical Polymerization of Methyl Methacrylate and Styrene Determined by the Reaction of Structurally Well-Defined Polymer End Radicals. *Macromolecules* **2015,** 48 (18), 6450-6456 DOI: 10.1021/acs.macromol.5b01532.
34. Nakamura, Y.; Lee, R.; Coote, M. L.; Yamago, S. Termination Mechanism of the Radical Polymerization of Acrylates. *Macromol. Rapid Comm.* **2016,** 37 (6), 506-513 DOI: https://doi.org/10.1002/marc.201500677.
35. Nakamura, Y.; Ogihara, T.; Hatano, S.; Abe, M.; Yamago, S. Control of the Termination Mechanism in Radical Polymerization by Viscosity: Selective Disproportionation in Viscous Media. *Chem. Eur. J.* **2017,** 23 (6), 1299-1305 DOI: 10.1002/chem.201604659.
36. Ribelli, T. G.; Rahaman, S. M. W.; Matyjaszewski, K.; Poli, R. Catalyzed Radical Termination in the Presence of Tellanyl Radicals. *Chem. Eur. J.* **2017,** 23, 13879 – 13882 DOI: https://doi.org/10.1002/chem.201703064.
37. Thevenin, L.; Fliedel, C.; Fantin, M.; Ribelli, T. G.; Matyjaszewski, K.; Poli, R. Reductive termination of cyanoisopropyl radicals by copper(I) complexes and proton donors:

organometallic intermediates or coupled proton-electron transfer? *Inorg. Chem.* **2019,** 58, 6445–6457 DOI: https://doi.org/10.1021/acs.inorgchem.9b00660.
38. Li, X. P.; Ogihara, T.; Abe, M.; Nakamura, Y.; Yamago, S. The Effect of Viscosity on the Diffusion and Termination Reaction of Organic Radical Pairs. *Chem. Eur. J.* **2019,** 25 (42), 9846-9850 DOI: 10.1002/chem.201902074.
39. Konkolewicz, D.; Wang, Y.; Zhong, M. J.; Krys, P.; Isse, A. A.; Gennaro, A.; Matyjaszewski, K. Reversible-Deactivation Radical Polymerization in the Presence of Metallic Copper. A Critical Assessment of the SARA ATRP and SET-LRP Mechanisms. *Macromolecules* **2013,** 46 (22), 8749-8772 DOI: 10.1021/ma401243k.
40. Pintauer, T.; Matyjaszewski, K. Structural aspects of copper catalyzed atom transfer radical polymerization. *Coord. Chem. Rev.* **2005,** 249 (11-12), 1155-1184.
41. Moad, G.; Solomon, D. H. *The Chemistry of free Radical Polymerization*. 2nd ed.; Elsevier: Amsterdam, 2005.
42. Moad, G. A Critical Assessment of the Kinetics and Mechanism of Initiation of Radical Polymerization with Commercially Available Dialkyldiazene Initiators. *Prog. Polym. Sci.* **2019,** 88, 130-188 DOI: 10.1016/j.progpolymsci.2018.08.003.
43. Barry, J. T.; Berg, D. J.; Tyler, D. R. Radical Cage Effects: Comparison of Solvent Bulk Viscosity and Microviscosity in Predicting the Recombination Efficiencies of Radical Cage Pairs. *J. Am. Chem. Soc.* **2016,** 138 (30), 9389-9392 DOI: 10.1021/jacs.6b05432.
44. Wakai, C.; Nakahara, M. Attractive potential effect on the self-diffusion coefficients of a solitary water molecule in organic solvents. *J. Chem. Phys.* **1997,** 106 (18), 7512-7518 DOI: 10.1063/1.473755.
45. Tang, W.; Matyjaszewski, K. Effect of Ligand Structure on Activation Rate Constants in ATRP. *Macromolecules* **2006,** 39 (15), 4953-4959.
46. Wulkow, M. Computer Aided Modeling of Polymer Reaction Engineering-The status of Predici, 1-Simulation. *Macromol. React. Engin.* **2008,** 2 (6), 461-494 DOI: https://doi.org/10.1002/mren.200800024.
47. Lorandi, F.; Fantin, M.; Isse, A. A.; Gennaro, A.; Matyjaszewski, K. New protocol to determine the equilibrium constant of atom transfer radical polymerization. *Electrochimica Acta* **2018,** 260, 648-655 DOI: https://doi.org/10.1016/j.electacta.2017.12.011.
48. Fischer, H.; Radom, L. Factors controlling the addition of carbon-centered radicals to alkenes-an experimental and theoretical perspective. *Angew. Chem. Int. Ed.* **2001,** 40 (8), 1340-1371 DOI: 10.1002/1521-3773(20010417)40:8<1340::aid-anie1340>3.0.co;2-#.
49. Zerk, T. J.; Gahan, L. R.; Krenske, E. H.; Bernhardt, P. V. The fate of copper catalysts in atom transfer radical chemistry. *Polym. Chem.* **2019,** 10, 1460-1470 DOI: https://doi.org/10.1039/c8py01688g.

TABLE OF CONTENT GRAPHIC.